Geomatics Research Australasia
No. 64, June 1996

GRAVIMETRIC GEOID REFINEMENT USING HIGH RESOLUTION GRAVITY AND TERRAIN DATA

Will E. Featherstone [1]
Ken Alexander [2]
Michael G. Sideris [3]

1. School of Surveying and Land Information
Curtin University of Technology
Perth, WESTERN AUSTRALIA

2. Survey Integration Services
Department of Land Administration
Midland, WESTERN AUSTRALIA

3. Department of Geomatics Engineering
The University of Calgary
Calgary, Alberta, CANADA

ABSTRACT

In regions where additional, spatially dense gravity and terrain information are available to augment existing data, a gravimetric determination of the geoid can be improved by incorporating these new data. In this study, 4,016 additional gravity observations, measured on a near-regular 2km by 3km grid in Western Australia have been used to compute a gravimetric geoid model using fast Fourier transform (FFT) techniques. A digital terrain model is also used during the geoid computations, which is derived from gravity station elevations and spot heights in the area. Using 21 spirit-levelled Australian Height Datum (AHD) heights in conjunction with Global Positioning System (GPS) ellipsoidal heights as control data, the standard deviation of the new gravimetric geoid is ±0.0824m. This represents a 31% improvement over the existing AUSGEOID93 gravimetric geoid and a 48% improvement over the OSU91A global geopotential model. Of these improvements, approximately 10% is due to the additional gravity data and approximately 1% is due to the terrain effects; the remainder is due to the dense gridding of the data prior to the FFT computations.

1. INTRODUCTION

The Global Positioning System (GPS) in its precise relative carrier-phase mode provides three-dimensional coordinates of latitude, longitude and ellipsoidal height relative to known fixed points in the World Geodetic System 1984 (WGS84). The horizontal coordinates (latitude and longitude) are applicable on any chosen datum after the use of standard coordinate transformations; see, for example, Defense Mapping Agency (1987) or Steed (1990). The ellipsoidal height must also be transformed to an orthometric height using a knowledge of the geoid-WGS84-ellipsoid separation at each GPS point (see equations 1 and 2).

The GPS ellipsoidal height is a purely geometrical quantity, which neglects the physical effects of the Earth's gravity field. The gravity vector provides the common experience of the vertical or plumb-line, which defines the horizontal and vertical orientation of most instruments used for surveying measurements. Under the influence of gravity, water that is free to move will flow from higher to lower elevations, but in a purely geometric system, the water may appear to flow from a point of lower ellipsoidal height to a point of higher ellipsoidal height. Therefore, orthometric heights, which refer to the geoid, must be used for virtually all practical surveying and engineering applications.

In Australia, the Australian Height Datum (AHD) height is related to the GPS-derived WGS84 ellipsoidal height at a point A by the following simple transformation:

$$H_A = h_A - N_A \qquad (1)$$

where: H_A is the AHD height of point A above the geoid,
h_A is the ellipsoidal height of point A above the WGS84 ellipsoid, and
N_A is the geoid-WGS84-ellipsoid separation at point A.

In the relative case, between two points A and B, this relationship becomes:

$$\Delta H_{AB} = \Delta h_{AB} - \Delta N_{AB} \qquad (2)$$

Therefore, given a change in ellipsoidal height (Δh) from relative GPS observations, the precision of the corresponding change in AHD height (ΔH) is controlled, in part, by the precision with which the change in the geoid-ellipsoid separation (ΔN) is known.

The gravimetric method provides a source of these geoid-ellipsoid separations with which to perform this coordinate transformation. Among many other factors, the accuracy of the gravimetric method is a function of the coverage, spatial density and accuracy of the gravity data used to compute the geoid undulations.

This paper describes the improvement in the gravimetric determination of the geoid in the Merlinleigh Basin, Western Australia, when spatially dense gravity and terrain data are used (cf. Parks and Milbert, 1995). This is evidenced by an improvement of GPS-derived AHD heights when compared to control AHD heights provided by conventional spirit-levelling.

2. THE AUSGEOID93 GRAVIMETRIC GEOID

The current gravimetric geoid model of Australia, which can be used to transform GPS heights to the AHD, is named AUSGEOID93 (Steed and Holtznagel, 1994). It was computed by the Australian Surveying and Land Information Group (AUSLIG), who combined the 1980 release of the Australian Geological Survey Organisation's (AGSO's) gravity data-base with the OSU91A global geopotential model (Rapp *et al.*, 1991) using the ring integration technique and computer algorithms of Kearsley (1988). The spatial density of the 1980 AGSO data used is ~11km (~7km in South Australia and Tasmania), with more detailed coverage in areas where surveys and traverses have been conducted, primarily for oil and mineral exploration. This data coverage infers that AUSGEOID93 models the geoid of Australia with wavelengths greater than ~20km in most land areas.

AUSLIG has taken responsibility for the dissemination of AUSGEOID93, which is usually supplied to users as a pre-gridded set of geoid-WGS84-ellipsoid separations with a 10' by 10' spacing in WGS84 latitude and longitude. Therefore, AUSGEOID93 in this standard form can only be expected to represent Australian geoid undulations with a wavelength greater than ~40km. The absolute accuracy of AUSGEOID93 is estimated to be ±0.3m (Steed and Holtznagel, 1994), whilst the relative precision has been estimated at 2-5mm/km (Kearsley and Govind, 1991; Steed and Holtznagel, *ibid.*; Featherstone and Alexander, 1996). In areas where AUSGEOID93 is smooth and well determined, this relative precision can increase to 0.1-1mm/km, but in areas where the geoid is irregular (usually in areas of rugged terrain or rapidly varying gravity), the

precision can decrease to 4-5mm/km. However, these estimates of accuracy and precision are made using GPS heights and AHD heights as control data, which have their own error budgets.

The gravimetric method can be assumed to model the geoid at wavelengths greater than the resolution of the terrestrial gravity (and terrain) data used in its computation. In the Merlinleigh Basin area of Western Australia, spatially dense gravity and terrain data have been used to increase the fidelity of the geoid down to wavelengths greater than ~6km. Accordingly, the use of these additional data in the geoid computations are expected to produce a gravimetric geoid which improves upon the existing AUSGEOID93 in the Merlinleigh Basin area.

3. SOME RELEVANT CONCEPTS IN PHYSICAL GEODESY

The basic relationship among the Earth's gravity field (g), orthometric height (H) and gravity potential (W) is given by the following total derivative (Heiskanen and Moritz, 1967 p.50):

$$dW = -g\, dH \tag{3}$$

As the Earth's gravity field is spatially variant, so must be the relationship between W and H. This explains why a spirit-levelling loop, assumed to be error-free, will not close. The geoid is the particular equipotential surface (W = constant) of the Earth's gravity field which most closely corresponds with the mean surface of the open oceans. It is also a closed and continuous surface which undulates in an irregular fashion because of mass density variations within the Earth.

To determine the geoid using the gravimetric method, gravity observed on the Earth's surface must first be reduced to the geoid by accounting for the observation elevation, whilst preserving the Earth's mass. In modern geoid determination, the Faye gravity anomaly (Δg) is used, which is computed by adding the gravimetric terrain correction to the free-air gravity anomaly:

$$\Delta g = \Delta g_{\mathrm{FA}} + C \tag{4}$$

where: Δg_{FA} is the second-order free-air gravity anomaly, computed using the procedures described in Featherstone (1995), and

C is the gravimetric terrain correction (Moritz, 1968):

$$C = \frac{G\rho R^2}{2}\int_{\sigma}\frac{(H'-H)^2}{l^3}d\sigma \tag{5}$$

where: G is the Newtonian gravitational constant,

ρ is the topographic density, assumed to be a constant 2670kgm^{-3},

R is the mean radius of the Earth,

H is the height of the computation point,

H' is the height of each distant point,

l is their separation, and

$d\sigma$ is an integration element on the sphere.

The fundamental relationship between the geoid height (N) and gravity anomalies (Δg) is given by Stokes's formula (Heiskanen and Moritz, 1967 p.95). However, this formula requires that gravity data are used over the entire Earth, which is an onerous condition that is not currently satisfied. Instead, a remove-restore approach is adopted, which significantly reduces the data and computational requirements. It also reduces the effect of the spherical approximations inherent to Stokes's formula (*ibid.*). During this remove-restore approach, a global geopotential model (GGM) provides the long wavelength geoid undulations and Stokes's formula adds those wavelengths greater than that implied by the resolution of the gravity and terrain data. In mathematical form, Stokes's formula in conjunction with the remove-restore technique is given by:

$$N = N_{GGM} + \frac{R}{4\pi\gamma}\int_{\sigma} S(\psi)(\Delta g - \Delta g_{GGM})\,d\sigma \tag{6}$$

$$N_{GGM} = \frac{GM}{r\gamma}\sum_{n=2}^{M\max}\left(\frac{a}{r}\right)^n\sum_{m=0}^{n}(\delta\overline{C}_{nm}\cos m\lambda + \overline{S}_{nm}\sin m\lambda)\,\overline{P}_{nm}(\cos\theta) \tag{7}$$

$$\Delta g_{GGM} = \frac{GM}{r^2}\sum_{n=2}^{M\max}\left(\frac{a}{r}\right)^n(n-1)\sum_{m=0}^{n}(\delta\overline{C}_{nm}\cos m\lambda + \overline{S}_{nm}\sin m\lambda)\,\overline{P}_{nm}(\cos\theta) \tag{8}$$

where: γ is mean normal gravity,

$S(\psi)$ is Stokes's function or a modification thereof,
Δg are the Faye (terrain corrected free-air) gravity anomalies,
ψ is the angular distance from the computation point to the roving point,
GM is the geocentric gravitational constant,
(r,θ,λ) are the spherical polar coordinates of the computation point,
$\overline{P}_{nm}$ are the fully normalised associated Legendre polynomials for degree n and order m, and
$\delta\overline{C}_{nm}$ and $\overline{S}_{nm}$ are the fully normalised spherical harmonic coefficients of the GGM, which have been reduced by the even zonal harmonics of the reference ellipsoid, and are complete to degree and order M_{max}.

As equation (6) uses Faye gravity anomalies, this produces a Faye co-geoid which must be converted to the 'true' geoid by adding the indirect effect (N_i) corresponding to the free-air reduction and gravimetric terrain correction. This indirect effect is given by Wichiencharoen (1982) as:

$$N_i = -\frac{\pi G\rho H^2}{\gamma} - \frac{G\rho R^2}{6\gamma}\int_{\sigma}\frac{(H'^3 - H^3)}{l^3}d\sigma \qquad (9)$$

where all symbols have been defined previously.

4. THE DETAILED GPS AND GRAVITY SURVEYS

In the Merlinleigh Basin area of Western Australia, the AGSO gravity data coverage has been supplemented over a ~20,000 square kilometre area with 4,016 point gravity observations, established on a near-regular 2km by 3km grid (see Figure 1). The gravity survey was conducted by Haines Surveys Pty Ltd on behalf of the Geological Survey of Western Australia, as part of its petroleum initiatives programme. The size (approximately 255km by 45-120km), shape (irregular polygon) and azimuth (335°) of the survey area were selected so as to optimise subsequent geophysical interpretations, and not for gravimetric geoid refinement. Nevertheless, these data provide a useful source of gravity and terrain information for gravimetric geoid computations.

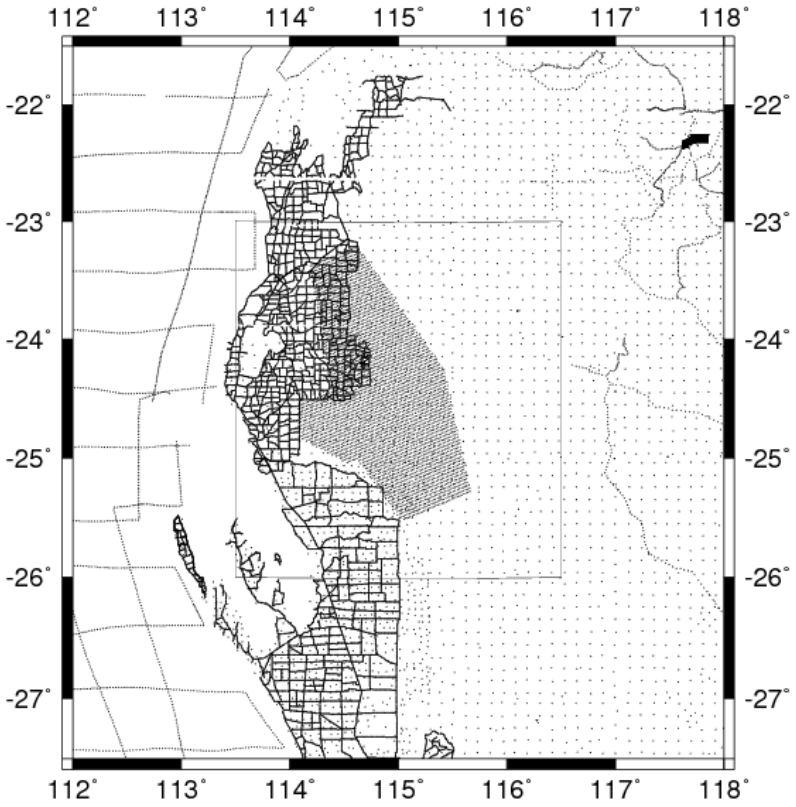

Figure 1. The coverage of the Merlinleigh Basin gravity survey (central polygon) in relation to the 1992 release of the AGSO gravity data-base. The inner rectangle shows the extent of the gravimetric geoid solution. (Mercator projection).

The survey specifications dictated that each gravity observation have a positional accuracy relative to the Australian Geodetic Datum 1984 (AGD84) and Australian Height Datum (AHD) of ±0.3 metres at the confidence level of one standard deviation (1σ). The gravity observation requirements were specified to have an accuracy of ± 0.05mgal relative to the ISOGAL84 base-station network (Wellman *et al.*, 1985), also at the 1σ confidence level. Conversely, the AGSO gravity observations used to compute AUSGEOID93 are estimated to have an uncertainty of ±0.3mgal (Barlow, 1977) and the elevations, most of which were derived using barometric levelling, are estimated to have an uncertainty of ±4-6m (Leaman, 1984). Therefore, these new gravity data represent a considerable improvement over the existing AGSO gravity data in terms of spatial density, spatial homogeneity and accuracy. Moreover, they provide test data for assessing the increase in precision that could be expected in future Australian gravimetric geoids through the inclusion of improved data.

A coarse prediction of the improvements expected in the determination of the Merlinleigh Basin gravimetric geoid can be made by comparing the accuracy of the existing AGSO data and the new gravity data. The estimates of gravity observation and elevation uncertainties are propagated to the free-air gravity anomaly. In the case of the AGSO data, this infers an error in the free-air anomaly of approximately ±1.3-1.9mgal, whereas for the new data, the error is approximately ±0.2mgal. This corresponds to an 85-90% improvement in the accuracy of the free-air gravity anomalies. Despite this, a commensurate level of improvement is not expected in the gravimetric geoid because of the many other factors that affect practical geoid computation and its subsequent analysis using GPS and spirit-levelling data.

4.1 Survey Techniques

The contracted gravity survey established 14 new gravity base-stations connected to the existing AGD84 geodetic and ISOGAL84 gravity networks. These base-stations were then used to control both the GPS positioning and the gravimeter drift during the surveys. The primary observational equipment used throughout the survey consisted of two *Trimble Land Surveyor II* single-frequency carrier-phase GPS receivers, a *Scintrex CG-3 Autograv* digital gravimeter, and associated post-processing softwares.

For the geodetic establishment of the 14 base-stations, 49 static, relative carrier-phase GPS baselines were observed for a minimum duration of four hours over baseline lengths averaging less than 40km (shortest line 7km, longest line 70km). The network was geometrically well conditioned with connections to 12 existing AGD84 geodetic stations. This configuration provided considerable redundancy and allowed assessment by least squares adjustment and analysis. The accuracy achieved for the GPS-derived control was better than 2mm/km (ppm) horizontally relative to the AGD84, and agreed with spirit-levelled AHD heights to a standard deviation of ±0.116m (cf. Table 2) when using bi-cubically interpolated AUSGEOID93 geoid heights. This GPS network analysis was based on holding the horizontal coordinates and ellipsoidal height (derived from AUSGEOID93 and a spirit-levelled AHD height) fixed at the northernmost first-order geodetic control station, which is also one of the ISOGAL84 gravity base-stations in the Merlinleigh Basin region.

The gravity control at the 14 new base-stations was provided using two Scintrex gravimeters at different epochs. Each gravimeter independently observed two sets of readings at every base-station. Then, gravimetric connections were made to two ISOGAL84 stations in the region (A47 and Carnarvon; Wellman *et al*., 1985), so as to convert the relative gravimeter observations to absolute gravity values. Again, redundancy of observations existed, thus allowing least squares estimation of the absolute gravity value for each base-station and the accuracy attained. The results from the final adjustment indicated that the gravity base-station network achieved an accuracy of better than ±0.05mgal (Haines Surveys P/L, 1995).

The analysis of the 245 repeat gravity and GPS stations, listed in Table 1, gives an indication of the precision of the gravity and GPS survey relative to the 14 base-stations. These data suggest that the survey met its original specifications.

Table 1. Estimated GPS and gravity survey precision based on a comparison of 245 repeat observations (from Haines Surveys P/L, 1995).

differences	*UTM easting (m)*	*UTM northing (m)*	*ellipsoidal height (m)*	*observed gravity (mgal)*
mean	0.005	–0.029	0.053	0.030
std. devn.	0.043	0.029	0.010	0.004
minimum	0.000	0.001	0.000	0.000
maximum	0.297	0.385	0.249	0.188

The majority of gravity stations were accessed using a helicopter, and navigation to each pre-determined latitude and longitude used absolute C/A-code GPS (±100m). The GPS and gravity data were observed simultaneously at each station. Post-processed, carrier-phase kinematic GPS techniques then provided WGS84 three-dimensional positions at each site. The complete survey took 12 weeks (83 days) in the field, including the establishment of all horizontal, vertical and gravity control stations, the observation of 245 repeat stations for quality control purposes, and 17 ‘stand-by’ days for helicopter maintenance, rain, etcetera (Haines Surveys P/L, 1995). These figures indicate an all-inclusive, average survey rate of 48 completed gravity

observations per day, which is far more productive than could be expected using conventional surveying techniques and ground-based transportation in this area.

5. THE GRAVIMETRIC GEOID COMPUTATIONS

The terrestrial gravity and terrain data used to compute the Merlinleigh Basin gravimetric geoid were taken from a 6° by 6° area bound by longitude 112°E to 118°E and latitude 21° 30'S and 27° 30'S and comprise:

- 4,016 new gravity observations, horizontal positions and GPS-derived AHD heights on a near-regular 2km by 3km grid over the Merlinleigh Basin (Figure 1). The AHD heights of these new stations were derived using AUSGEOID93 geoid heights bi-cubically interpolated from the standard 10' by 10' grid.
- 23,497 gravity observations from the 1992 release of the Australian Geological Survey Organisation's (AGSO's) gravity data-base. These are predominantly at a spacing of ~11km, with a higher spatial density in the West of the study area due to geophysical prospecting for petroleum (see Figure 1).
- A digital terrain model (DTM) created from a combination of 204,860 spot heights from the Australian Surveying and Land Information Group's (AUSLIG's) data-base, the 23,497 elevations provided with the AGSO gravity stations, and the GPS-derived AHD heights at each of the 4,016 gravity survey points. A grey-scale image of the DTM is shown in Figure 2 where the heights range from sea-level (black) to 1199m (white).
- 130,676 fully normalised spherical harmonic coefficients which define the OSU91A global geopotential model (Rapp *et al.*, 1991) complete to spherical harmonic degree and order 360.

5.1 Data Pre-processing and Gridding

All gravity and terrain data pre-processing followed the procedures described in Featherstone (1995). This involved transforming their horizontal coordinates to WGS84 using a seven-parameter transformation, computing free-air gravity anomalies using a second-order free-air reduction, applying atmospheric corrections, and evaluating normal gravity with Somigliana's closed formula. This approach avoids the propagation of coordinate-related errors into the gravity anomalies and terrain data, and hence the gravimetric geoid.

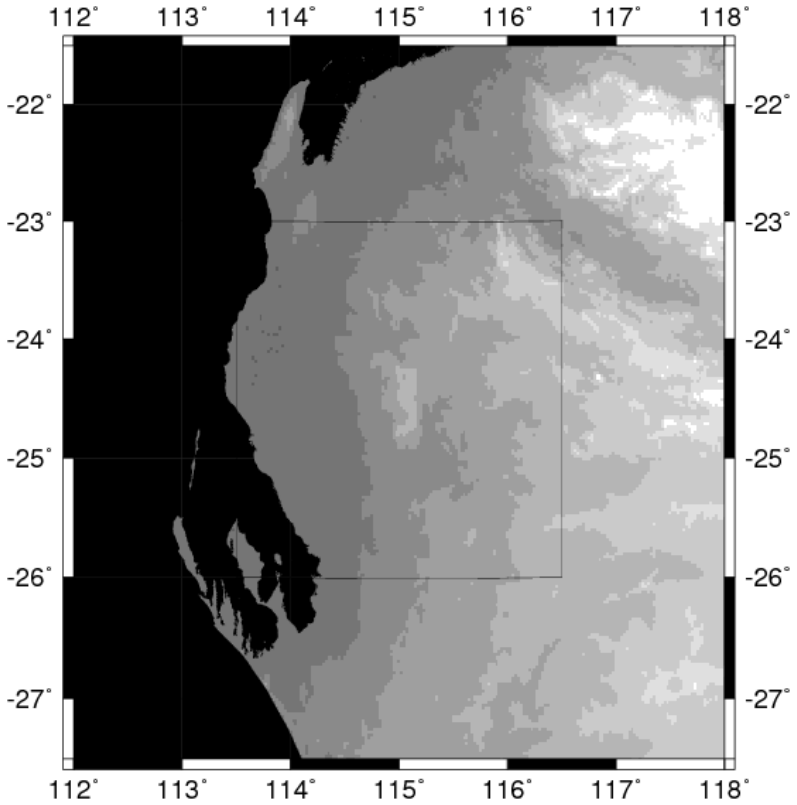

Figure 2. A grey-scale image of the Merlinleigh Basin DTM. Elevations are in 200m bins from 0m (black) to 1200m (white). The inner rectangle shows the extent of the gravimetric geoid solution. (Mercator projection).

The computational procedure used in this study is the fast Fourier transform (FFT). The FFT approach to gravimetric geoid computation requires a regular grid of gravity and terrain data. Therefore, the discrete gravity observations and spot heights were interpolated onto a 1.5' by 1.5' grid, which is commensurate with the resolution of the Merlinleigh Basin gravity survey. Firstly, the gravity anomalies implied by the degree-360 expansion of the OSU91A global geopotential model (equation 8) were subtracted point-by-point from all terrestrial free-air gravity anomalies using the routines of Rapp (1982). This procedure produced residual free-air gravity anomalies. The OSU91A model was chosen because this has previously been shown to be the best fit to the geoid and gravity field in Australia (Zhang and Featherstone, 1995).

It is common practice to also remove the gravimetric effect of the terrain, via the complete Bouguer reduction, prior to interpolation and gridding so as to avoid aliasing

of the short wavelength gravity features. However, in this region of Australia, the Bouguer gravity anomalies are not necessarily smooth and are more sensitive to aliasing and thus less suitable for interpolation than the free-air gravity anomalies (Featherstone *et al.*, 1995). Therefore, the interpolation and gridding were performed using the residual free-air gravity anomalies.

A surface fitting technique, based on the minimum tension spline algorithm of Smith and Wessel (1990), was used to interpolate the residual gravity data onto the 1.5' by 1.5' grid. This routine is readily available in version 3.0 of the *GMT* (Generic Mapping Tools) software of Wessel and Smith (1995). The 1.5' by 1.5' DTM was created using the same gridding algorithm and used elevation data from the AUSLIG spot heights and the gravity station elevations.

In Figure 3, the extent of gravity and terrain data used to compute the Merlinleigh Basin gravimetric geoid cover a larger area than the geoid solution itself. This increased data area is chosen so as to minimise any gravimetric geoid errors induced by data-related edge effects. These arise when gravity data containing wavelengths shorter than those specified by the OSU91A global geopotential model, are omitted from a boundary outside the area over which the geoid is desired. The extent of this boundary is controlled by the maximum degree of the global geopotential model, which is 30' or approximately 55km for the degree 360 expansion of OSU91A. In this study, the data area has been extended by 1.5° so as to ensure that these data-related edge effects do not contaminate the geoid solution.

The resulting residual gravimetric geoid undulations are assumed to supply all wavelengths less than the dimension of the data area (6° or ~600km), and greater than twice the resolution of the gravity and terrain data (3' or ~6km). Furthermore, an additional 3° (or 50%) of zero padding was added to each edge of the data grids in order to remove the windowing and edge effects associated with the FFT (Sideris and Li, 1993).

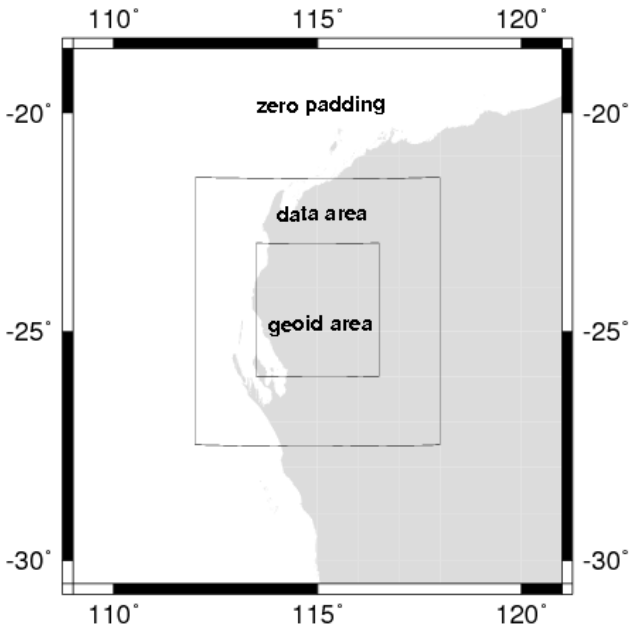

Figure 3. The extent of the gravimetric geoid solution in relation to the gravity and terrain data area, and the additional 50% zero padding required for the FFT computations. (Mercator projection)

Two primary data sets in the area between longitude 112°E to 118°E and latitude 21° 30'S and 27° 30'S were used to compute two gravimetric geoid models in order to assess any improvements due to the inclusion of high resolution gravity and terrain data. These are:

1. A 1.5' by 1.5' grid of residual free-air gravity anomalies, interpolated from the AGSO gravity data only, together with a 1.5' by 1.5' digital terrain model (DTM) interpolated from the AUSLIG spot heights and the AGSO gravity station elevations only.
2. A 1.5' by 1.5' grid of residual free-air gravity anomalies, interpolated from the AGSO gravity data and the Merlinleigh Basin gravity survey data, and a 1.5' by 1.5' DTM, interpolated from the AUSLIG spot heights, AGSO station elevations, and the GPS-derived station elevations from the Merlinleigh Basin gravity survey.

A direct comparison of these two geoid solutions will show any improvement in the gravimetric determination of the Merlinleigh Basin geoid as a result of the inclusion of the additional dense gravity data. Moreover, when each of these geoid solutions is

compared with the existing AUSGEOID93, this will illustrate any improvement resulting from the inclusion of the 1992 AGSO gravity data and a high resolution DTM. (Recall that AUSGEOID93 only uses the 1980 AGSO gravity data with no additional terrain information.)

5.2 The Fast Fourier Transform (FFT) Algorithms

The geoid computations in this study were conducted entirely in the frequency domain via the fast Fourier transform. The geoid undulations implied by the OSU91A global geopotential model were computed from the spherical harmonic series in equation (7) using the algorithms and software of Rapp (1982). The residual geoid undulations from Stokes's formula (the third term in equation (6)) were computed using the one-dimensional FFT method (Haagmans *et al*., 1993). This is reported to produce results identical to numerical integration of Stokes's formula when using identical input gravity data, without the need for planar, or any other, FFT-related approximations. The 1D-FFT equivalent of equation (6) is:

$$N = N_{GGM} + \frac{R\Delta\phi\,\Delta\lambda}{4\pi\gamma}\mathbf{F}^{-1}\left[\left\{\sum \mathbf{F}\left\{S(\psi)\right\}\mathbf{F}\left\{(\Delta g - \Delta g_{GGM})\cos\phi\right\}\right] \qquad (10)$$

where: $\Delta\phi$ and $\Delta\lambda$ are the grid spacing in latitude and longitude respectively;

F and $\mathbf{F}^{-1}$ are the one-dimensional Fourier transform and its inverse respectively, which are performed in the longitudinal direction; and

Σ is the summation, which is performed in the latitudinal direction.

The gravimetric terrain correction (equation 5) and the indirect effect (equation 9) were also computed using their respective 1D-FFT counterparts (Sideris and She, 1995; Li and Sideris, 1994), viz.

$$C = \frac{G\rho R^2}{2}\left(\mathbf{F}^{-1}\left[\left\{\sum \mathbf{F}\left\{1/l^3\right\}\mathbf{F}\left\{H'^2\right\}\right] - 2H\mathbf{F}^{-1}\left[\left\{\sum \mathbf{F}\left\{1/l^3\right\}\mathbf{F}\left\{H'\right\}\right]\cdots\right.\right.$$

$$\left.\left. + H^2\mathbf{F}^{-1}\left[\left\{\sum \mathbf{F}\left\{1/l^3\right\}\mathbf{F}\{1\}\right]\right)\right. \qquad (11)$$

$$N_i = -\frac{\pi G\rho}{\gamma} H^2 + \frac{G\rho\Delta\phi\,\Delta\lambda}{6\gamma}\left(H^3\mathbf{F}^{-1}\left[\left\{\sum \mathbf{F}\left\{1/l^3\right\}\mathbf{F}\{1\}\right\}\right]\right.$$
$$\left. + \mathbf{F}^{-1}\left[\left\{\sum \mathbf{F}\left\{1/l^3\right\}\mathbf{F}\left\{H'^3\right\}\right\}\right]\right) \qquad (12)$$

where all symbols have been defined previously.

The FFT approach to gravimetric geoid computation provides time efficiencies compared to numerical integration with identical results, provided that all data are used from the same grid. The computations were performed using the University of Calgary's FFT software. More details of this software and numerical results of the application of Fourier techniques to geoid and gravimetric terrain correction computations and can be found in Sideris (1994 and 1995) and Sideris and She (1995).

In this study, the geoid was computed in several component parts, which were subsequently added to provide the total geoid height. The residual free-air co-geoid undulations were computed by using the residual free-air gravity anomalies in equation (10). The gravimetric terrain corrections were computed using the DTM in equation (11). These gravity values were then used in equation (10) to evaluate the corresponding effect on the geoid. When the free-air co-geoid and topographic geoid effect were added, this produced the Faye co-geoid. The indirect effect was computed using the DTM in equation (12), and added to the Faye co-geoid to give the residual geoid undulations. Finally, the geoid undulations implied by the OSU91A model to degree and order 360 (equation 7) were restored to produce the total gravimetric geoid for the Merlinleigh Basin area.

These procedures were followed for both data-sets (ie. with and without the new data). Figure 4 shows the gravimetric geoid of the Merlinleigh Basin computed from all available gravity and terrain data (ie. with the new data).

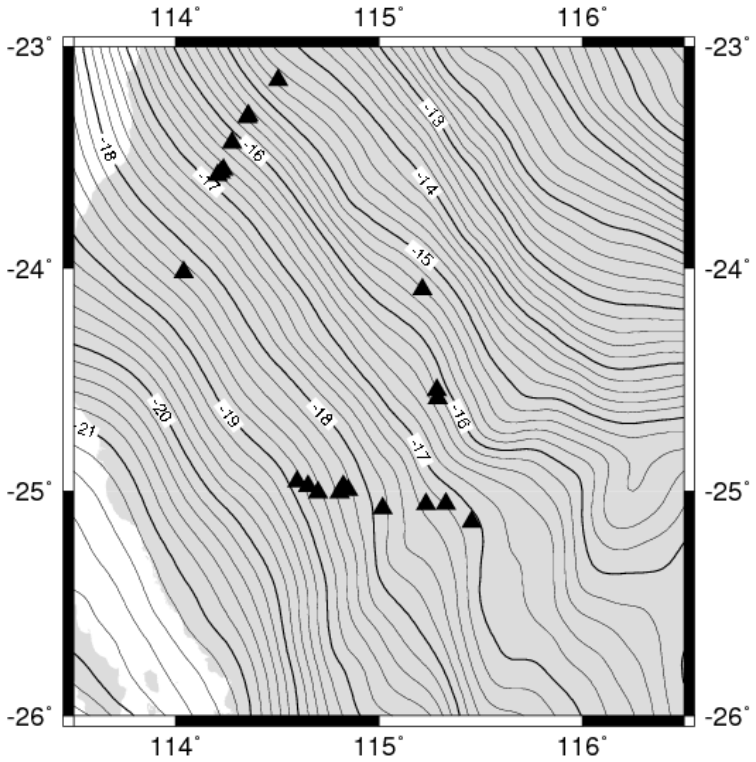

Figure 4. The Merlinleigh Basin gravimetric geoid computed from all available data via the FFT, together with the distribution of the 21 GPS-AHD control stations (Mercator Projection. Contours in metres relative to WGS84)

6. COMPARISONS WITH GPS AND LEVELLING DATA

The geometrical control data used to assess the precision of the gravimetric geoid solutions in the Merlinleigh Basin area were provided by existing AHD benchmarks, which had been occupied with static, relative carrier-phase GPS during the surveys (cf. equation 1). These control data comprise 24 discrete geoid heights, 21 of which are spirit-levelled and three of which have heights derived from the less accurate method of vertical angles. Therefore, two sets of statistical comparisons are given in Table 2; those for all 24 control stations, and those for the 21 spirit-levelled stations. In all comparisons, the control geoid heights have been subtracted from the gravimetric geoid heights.

The verification of any improvement in the precision of the gravimetric geoid solution will be seen in the standard deviations, with a smaller value indicating an improvement in the determination of the geoid. However, when all 24 control stations are included in the statistical analysis, there is no clear trend in the standard deviations in Table 2, because the large differences at the three trigonometric stations obscure the smaller differences at the spirit-levelled stations. Therefore, a comparison of the standard deviations at the 21 spirit-levelled stations only will indicate any improvements in the determination of the geoid using different approaches.

Only the standard deviation is used to give an indication of the relative precision of each solution because any gravimetric determination of the geoid is deficient in the zero- and first-degree terms, which manifest as a bias over this study area. Therefore, the mean differences are essentially meaningless when used to assess the precision of the geoid. This is also evidenced in Table 2, where the mean difference alone for the 21 levelled control stations would imply that OSU91A is the superior geoid model in this region, which would otherwise be unexpected because all other solutions include additional data.

Seven different geoid solutions were compared by subtracting the geometrically determined geoid heights from the gravimetric geoid heights and determining the maximum, minimum, mean, and standard deviation of these differences using *Microsoft Excel* (version 5.0) software. Also, geoid heights were computed from the OSU91A global geopotential model alone, and interpolated from the AUSGEOID93 grid. This allowed comparison of the new gravimetric geoid models with the two existing geoid models in the Merlinleigh Basin area.

The effect of including terrain data in the geoid solutions was also investigated by computing statistics which include and exclude the gravimetric terrain correction (equations 5 and 11) and indirect effect (equations 9 and 12), cumulatively referred to as the topographic effects. The AUSGEOID93 gravimetric geoid is a free-air co-geoid because neither gravimetric terrain corrections nor indirect effects were used during its computation (Steed and Holtznagel, 1994; Featherstone and Alexander, 1996). Therefore, the effect of neglecting topographic effects in the AUSGEOID93 and FFT geoid solutions can also be evaluated in the Merlinleigh Basin area.

Table 2. Differences between gravimetric geoid heights and the geometrical control stations for: OSU91A alone; AUSGEOID93 alone, an FFT geoid computed from the AGSO gravity data (FFT) alone, an FFT geoid computed from the AGSO and Merlinleigh gravity data (FFT(M)); and, the latter three geoid solution types but now including topographic effects. (All units are in metres.)

		no topographic effects			*inc. topographic effects*		
	OSU91	*AG93*	*FFT*	*FFT(M)*	*AG93*	*FFT*	*FFT(M)*
21 points							
mean	0.000	0.014	-0.120	-0.091	-0.027	0.132	0.103
std. devn.	0.1585	0.1190	0.0911	0.0827	0.1185	0.0908	0.0824
min.	-0.377	-0.303	-0.265	-0.219	-0.211	-0.092	-0.095
max.	0.221	0.199	0.105	0.107	0.288	0.276	0.178
24 points							
mean	-0.042	-0.037	-0.076	-0.051	0.024	0.088	0.063
std. devn.	0.5279	0.5424	0.5436	0.5295	0.5424	0.5434	0.5294
min.	-1.607	-1.589	-1.807	-1.761	-1.617	-1.452	-1.429
max.	1.560	1.602	1.464	1.441	1.575	1.819	1.773

The statistics in Table 2 are divided into three broad geoid solution types. The first column represents the geoid height differences for OSU91A alone. The next three columns give the geoid height differences computed without topographic effects. These comprise: AUSGEOID93, an FFT solution using the 1992 AGSO data alone, and an FFT solution using both the 1992 AGSO gravity data and the new Merlinleigh Basin gravity survey. The last three columns summarise the same solution types as above, but now with the topographic effects included. Of these, the last column gives the differences for the new Merlinleigh Basin gravimetric geoid, which has been computed using all available gravity and terrain data. The differences between the new gravimetric geoid and the 21 control stations are contoured in Figure 5 using the minimum tension spline algorithm supplied with the *GMT* software.

In Table 3, the standard deviations for the 21 sprit-levelled control stations in Table 2 have been summarised in terms of percentage improvements over the existing OSU91A and AUSGEOID93 geoid models. This gives a clearer indication of the

relative improvements gained by using the FFT approach, the use of topographic effects (gravimetric terrain corrections and indirect effects together), and the inclusion of the Merlinleigh Basin gravity survey data. The notation used in Table 3 is consistent with that of Table 2.

Table 3. Percentage improvements of the standard deviations between gravimetric and control geoid heights in relation to the existing OSU91A and AUSGEOID93 geoid models. (All units are in metres.)

	no topographic effects			*inc. topographic effects*		
	AG93	*FFT*	*FFT(M)*	*AG93*	*FFT*	*FFT(M)*
OSU91A	24.9%	42.5%	47.8%	25.2%	42.7%	48.0%
AG93	--	23.4%	30.5%	0.5%	23.7%	30.8%

6.1 Discussion

When comparing standard deviations at the 21 spirit-levelled stations in Tables 2 and 3, AUSGEOID93 alone performs 24.9% better than OSU91A alone ($\sigma = \pm 0.1190$m for AG93 versus $\sigma = \pm 0.1585$m for OSU91A), which is expected because of the use of Australian gravity data in the determination of AUSGEOID93. More interestingly, however, is the improvement achieved over AUSGEOID93 by using the FFT with what are essentially the same Australian gravity data ($\sigma = \pm 0.$ 1190m for AG93 versus $\sigma = \pm 0.0911$m for FFT, or 23.4%). In theory, the ring integration (AUSGEOID93) and FFT approaches to solving Stokes's formula should give the same results when using the same input gravity data. Therefore, this observed difference is due to the different pre-processing and gridding procedures used for the gravity data in each approach. The improved comparisons for the FFT approach thus vindicate the gravity reduction procedures of Featherstone (1995) and the use of a spline-interpolated 1.5' by 1.5' residual free-air gravity grid in this instance.

On adding the Merlinleigh Basin gravity data to the FFT solution an ignoring topographic effects for the moment, the improvement is relatively small ($\sigma = \pm$ 0.0911m for FFT versus $\sigma = \pm 0.0827$m for FFT(M), or 9.2%) when considering that the accuracy of the new data is increased by 85-90% and the spatial density over most of the computation area is increased by approximately 70% (Figure 1). However, as

stated earlier, commensurate levels of improvement were not expected in the gravimetric geoid because of the many other factors that influence gravimetric geoid determination.

Another observation from the statistics in Tables 2 and 3 is the relatively small improvements gained by adding the topographical effects. For instance, applying the topographic corrections to the existing AUSGEOID93 only offers an improvement of 0.5% ($\sigma = \pm 0.1190$m versus $\sigma = \pm 0.1185$m). This is because the topography is relatively benign in the geoid computation area (see Figure 2) and thus does not have a significant effect on the gravimetric geoid computations. However, larger levels of improvement can be expected in those areas of Australia which exhibit more rugged terrain.

Overall, when including all available gravity and terrain data in the FFT geoid solution, the determination of the Merlinleigh Basin gravimetric geoid improves upon OSU91A by 48.0% and upon AUSGEOID93 by 30.8%. Therefore, the use of high resolution grids of gravity and terrain data in conjunction with the one-dimensional FFT technique indeed offers an improved determination of the geoid over the existing AUSGEOID93.

6.2 Differences Between Gravimetric Geoid and Control Data

The differences between the Merlinleigh Basin gravimetric geoid and 21 spirit-levelled control stations is contour-plotted in Figure 5, where a combination of long and short wavelength differences are evident. The short wavelength differences are either due to errors in the existing spirit-levelling data, which was conducted to third-order standards, or due to localised errors in the gravity data or terrain data or both. The long wavelength discrepancy corresponds to approximately 3.5mm/km and is due to one, or all, of the following factors:

- long wavelength errors propagating from the OSU91A global geopotential model;
- long wavelength errors propagating from the terrestrial gravity and/or terrain data;
- long wavelength differences between the AHD and the geoid (Featherstone, 1995);
- errors in the GPS-derived ellipsoidal and spirit-levelled AHD control heights;
- the lack of gravity observations in the western region of the data area (cf. Figure 1).

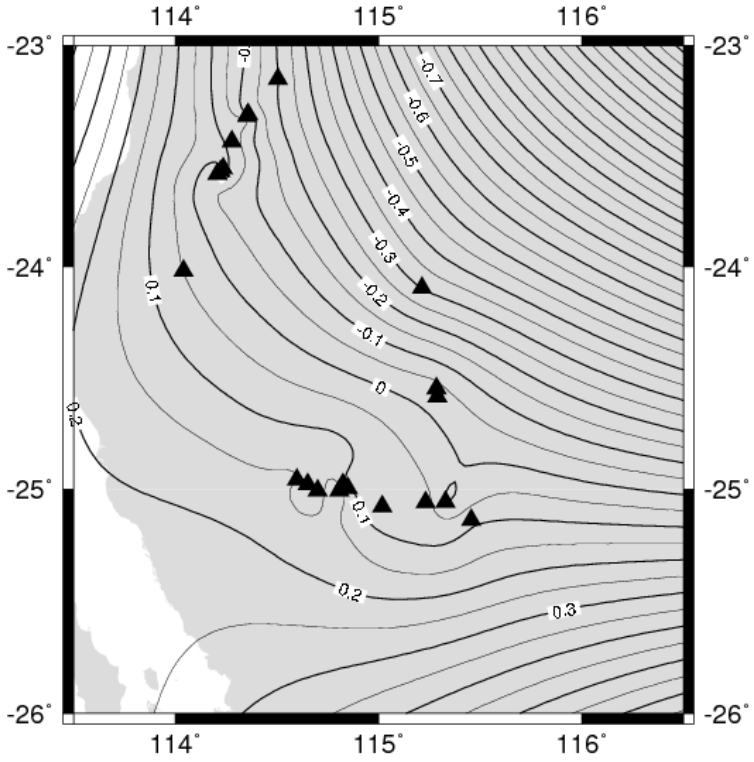

Figure 5. Differences between the Merlinleigh Basin gravimetric geoid and the 21 spirit-levelled control stations. (Mercator Projection. Contours in metres)

Of these error sources, the latter two provide the most likely explanation of these differences. Concerning the control data, the GPS network was held fixed in the vertical at the northernmost point only. This allows the ellipsoidal heights to effectively float about this point, and possibly introducing a long wavelength difference. A coarse estimate of the GPS error budget can be inferred from the network adjustment, which indicated a horizontal precision of 2mm/km. As GPS-derived heights are inherently 1.5 to 2 times less accurate than horizontal positions, this alone could account for the 3.5mm/km difference between the gravimetric and geometric geoid heights. Concerning the data coverage, the gravity observations are relatively sparse at sea (see Figure 1), which can introduce errors into the gravimetric geoid solution. Although the spline interpolation has provided estimates of the gravity anomalies in these areas, these values may not be representative of the actual gravity field. Therefore, the only approach to eliminate this effect is to collect more gravity data in these areas or supplement the existing marine gravity observations with those derived from satellite altimetry, for example.

However, it is difficult to prove conclusively that the GPS control and gravity data coverage are the only sources of this longer wavelength discrepancy; the most probable scenario is a combination of all five factors listed earlier. Nevertheless, this long wavelength difference can be eliminated by fitting a planar surface through the data, which removes the bias and the slope (cf. Sideris and She, 1995). Such an approach would produce a surface that is suitable for the direct determination of AHD heights from GPS in the Merlinleigh basin area (cf. Featherstone, 1996).

7. CONCLUSIONS AND RECOMMENDATIONS

The effects of including accurate, homogeneous and spatially dense gravity data in the determination of a gravimetric geoid using the 1D-FFT have been demonstrated by the improvements observed in the Merlinleigh Basin region of Western Australia. When using GPS and spirit-levelled data as a control on the new gravimetric geoid solution, the addition of these data provides an improvement of 30.8% over AUSGEOID93 alone and 48.0% over OSU91A alone.

The most significant proportion of this improvement was achieved through the use of the FFT algorithms in conjunction with a 1.5' by 1.5' grid of gravity data. This is because the interpolation of the existing gravity data onto a dense grid has reduced the discretisation error associated with the practical solution of Stokes's integral. The addition of the detailed Merlinleigh Basin gravity survey only provided ~10% of this improvement, whilst the addition of detailed terrain data only provided ~1% of the improvement. This relatively small improvement gained from the use of additional data indicates that the geoid in the Merlinleigh Basin area is well represented by the long wavelength features, and the addition of detailed gravity data or topographic effects does not provide significant benefits when compared to the increase in accuracy and resolution of the new gravity survey.

However, a long wavelength discrepancy of approximately 3.5mm/km remained between the new gravimetric geoid solution and geometrical control in the Merlinleigh Basin area. This is most probably due to a tilt in the GPS control network or the lack of gravity data offshore. However, this geoid solution can be used for practical GPS applications with the use of a planar surface to model the residual bias and tilt. Further

work will concentrate on identifying the source of this long wavelength difference between the geoid and control data, without the need for using a planar surface. An iterative technique will also be tested, where the refined gravimetric geoid will be used to reduce the GPS-positioned gravity observations before undertaking successive gravimetric geoid computations.

ACKNOWLEDGEMENTS

The authors wish to thank: the Western Australian Department of Minerals and Energy for providing the data and report pertaining to the gravity survey in the Merlinleigh Basin; the Australian Geological Survey Organisation (AGSO) for providing the 1992 Australian gravity data-base; the Australian Surveying and Land Information Group (AUSLIG) for providing the digital spot height data; Professor Dick Rapp of the Ohio State University, USA, for providing the OSU91A geopotential coefficients; Richard Haines of Haines Surveys Pty Ltd for providing some GPS data for validation purposes and a useful discussion on the gravity data acquisition; and, the Western Australian Department of Land Administration for providing levelling data. We would also like to thank the editor, Associate Professor Bill Kearsley, for his constructive comments, which inspired further analysis of the data. This research is funded as part of an Australian Research Council (ARC) grant A49331318.

REFERENCES

Barlow, B.C., 1977. Data limitations on model complexity; 2-D gravity modelling with desk-top calculators. *Bulletin of the Australian Society of Exploration Geophysicists*, 8(4), 139-143.

Defense Mapping Agency, 1987. Department of Defense World Geodetic System 1984: its definition and relationships with local geodetic systems. *Technical Report 8350.2*, Defense Mapping Agency, Washington, USA.

Featherstone, W.E., Zhang, K.F. and Stewart, M.P., 1995. A study of the behaviour of the Earth's gravity field in Australia. *poster presented to the XXI IUGG General Assembly*, Boulder, Colorado, USA, June.

Featherstone, W.E., 1995. On the use of Australian geodetic datums in gravity field determination. *Geomatics Research Australasia*, 61, 17-36.

Featherstone, W.E. and Alexander, K., 1996. An analysis of GPS height determination in Western Australia. *Australian Surveyor*, 41(1): 29-34.

Featherstone, W.E., 1996. A practical recipe for determining AHD heights from GPS. *Proceedings of the 37 Australian Surveyors' Congress*, Perth, Australia, April.

Haagmans, R.R., de Min, E. and van Gelderen, M., 1993. Fast evaluation of convolution integrals on the sphere using 1D-FFT, and a comparison with existing methods for Stokes's integral. *Manuscripta Geodaetica*, 18(5), 227-241.

Haines Surveys Pty. Ltd., 1995. Merlinleigh Sub-Basin Gravity Survey. *Report to the Western Australian Department of Minerals and Energy*, Perth.

Heiskanen, W.H. and Moritz, H., 1967. *Physical Geodesy*, W.H. Freeman and Co., San Francisco, USA.

Kearsley, A.H.W., 1988. Tests on the recovery of precise geoid height differences from gravimetry. *Journal of Geophysical Research*, 93(B6), 6559-6570.

Kearsley, A.H.W. and Govind, R., 1991. Geoid evaluation in Australia: A status report. *The Australian Surveyor*, 36(1), 30-40.

Leaman, D.E., 1984. Notes on micro-barometer elevation determinations. *Exploration Geophysics*, 15(1), 53-59.

Li, Y.C. and Sideris, M.G., 1994. Improved gravimetric terrain corrections. *Geophysical Journal International*, 119(3), 740-752.

Moritz, H., 1968. On the use of the terrain correction in solving Molodenskii's problem. *Report 108*, Department of Geodetic Science and Surveying, Ohio State University, USA.

Parks, W. and Milbert, D.G., 1995. A geoid height model for San Diego County, California, to test the effect of densifying gravity measurements on accuracy of GPS-derived orthometric height. *Surveying and Land Information Systems*, 55(1), 21-38.

Rapp, R.H., 1982. A Fortran program for the computation of gravimetric quantities from high degree spherical harmonic expansions. *Report 334*, Department of Geodetic Science and Surveying, Ohio State University, USA.

Rapp, R.H., Wang, Y.M. and Pavlis, N.K., 1991. The Ohio State 1991 geopotential and sea surface topography harmonic coefficient models. *Report 410*, Department of Geodetic Science and Surveying, Ohio State University, USA.

Sideris, M.G. and Li, Y.C., 1993. Gravity field convolutions without windowing and edge effects. *Bulletin Géodésique*, 67(2), 108-118.

Sideris, M.G., 1994. Geoid determination by FFT techniques. *Lecture Notes*, International School for the Determination and Use of the Geoid, DIIAR, Politecnico di Milano, Italy, October.

Sideris, M.G., 1995. FFT geoid computations in Canada. in: *New Geoids in the World*, Special joint issue of BGI bulletin 77 and IGeS bulletin 4.

Sideris, M.G. and She, B.B., 1995. A new, high-resolution geoid for Canada and part of the US by the 1D-FFT method. *Bulletin Géodésique*, 69(2), 92-108.

Smith, W.H.F. and Wessel, P., 1990. Gridding with continuous curvature splines in tension. *Geophysics*, 55, 293-305.

Steed, J., 1990. A practical approach to transformation between commonly used reference systems. *The Australian Surveyor*, 35(3), 248-264; 35(4), 384.

Steed, J. and Holtznagel, S., 1994. AHD heights from GPS using AUSGEOID93. *The Australian Surveyor*, 39(1), 21-27.

Wellman, P., Barlow, B.C. and Murray, A.S., 1985. Gravity base-station network values. *Report 261*, Bureau of Mineral Resources (now Australian Geological Survey Organisation), Canberra, Australia.

Wessel, P. and Smith, W.H.F., 1995. New version of the Generic Mapping Tools released. *EOS, Transactions of the American Geophysical Union*, 72, 441,445-446.

Wichiencharoen, C. (1982) The indirect effects on the computation of geoid undulations. *Report 336*, Department of Geodetic Science and Surveying, Ohio State University, USA.

Zhang, K.F. and Featherstone, W.E., 1995. The statistical fit of high degree geopotential models. *Geomatics Research Australia*, 63, 1-18.